Journal of Controlled Release 164 (2012) 346–354

Contents lists available at SciVerse ScienceDirect

Journal of Controlled Release

journal homepage: www.elsevier.com/locate/jconrel

HPMA copolymer-doxorubicin conjugates: The effects of molecular weight and architecture on biodistribution and in vivo activity

Tomáš Etrych [a], Vladimír Šubr [a,*], Jiří Strohalm [a], Milada Šírová [b], Blanka Říhová [b], Karel Ulbrich [a,*]

[a] Institute of Macromolecular Chemistry, Academy of Sciences of the Czech Republic v.v.i., Heyrovský Sq. 2, 162 06 Prague 6, Czech Republic
[b] Institute of Microbiology, Academy of Sciences of the Czech Republic v.v.i., Vídeňská 1083, 142 20 Prague 4, Czech Republic

ARTICLE INFO

Article history:
Received 21 March 2012
Accepted 21 June 2012
Available online 30 June 2012

Keywords:
Drug delivery
Tumour accumulation
Body distribution
HPMA copolymers
Pharmacokinetics
Renal elimination

ABSTRACT

The molecular weight and molecular architecture of soluble polymer drug carriers significantly influence the biodistribution and anti-tumour activities of their doxorubicin (DOX) conjugates in tumour-bearing mice. Biodistribution of *N*-(2-hydroxypropyl)methacrylamide (HPMA) copolymer-DOX conjugates of linear and star architectures were compared in EL4 T-cell lymphoma-bearing mice. Biodistribution, including tumour accumulation, and anti-tumour activity of the conjugates strongly depended on conjugate molecular weight (MW), polydispersity, hydrodynamic radius (R_h) and molecular architecture. With increasing MW, renal clearance decreased, and the conjugates displayed extended blood circulation and enhanced tumour accumulation. The linear conjugates with flexible polymer chains were eliminated by kidney clearance more quickly than the highly branched star conjugates with comparable MWs. Interestingly, the data suggested different mechanisms of renal filtration for star and linear conjugates. Only star conjugates with MWs below 50,000 g.mo^{-1} were removed by kidney filtration, while linear polymer conjugates with MWs near 70,000 g.mol^{-1}, exceeding the generally accepted limit for renal elimination, were detected in the urine 36–96 h after injection. Additionally, survival of tumour-bearing mice was strongly dependent on molecular weight and polymer conjugate architecture. Treatment of mice with the lower MW conjugate at a dose of 10 mg DOX eq./kg resulted in 12% long-term surviving animals, while treatment with the corresponding star conjugate enabled 75% survival of animals.

1. Introduction

Contemporary oncology is a fast-developing branch of medicine that exploits research achievements in other disciplines such as cell biology, immunology, and genetics. Additionally, polymer chemistry offers powerful tools for the development of new generations of drugs. Novel polymer drug delivery systems (DDS) have been developed and tested in numerous preclinical and clinical studies. The design of new polymer-drug conjugates is based on the idea that synthetic polymer carriers [1–3] can enable passive and active tumour-specific drug delivery. Conjugation of a chemotherapeutic agent to a hydrophilic polymer carrier increases the solubility of water-insoluble drugs, prolongs the circulation of a polymer-drug conjugate in the blood, influences drug pharmacokinetics and biodistribution, decreases side-toxicity and induces therapy-dependent cancer resistance as it was evidenced for HPMA copolymers of various structures earlier [4,5].

The Enhanced Permeability and Retention Effect (EPR) described by Maeda and Matsumura is based on the preferential accumulation of high-molecular weight (HMW) polymer drug conjugates in solid tumours, and the efficiency of this accumulation is molecular weight-dependent [6–8]. Furthermore, fluid-phase and receptor-mediated pinocytosis are the most important mechanisms underlining subsequent uptake of water-soluble polymer drug conjugates in target tumour cells.

The balance between elimination of polymeric drugs from the bloodstream by the kidneys, liver and other organs and extravasation from the blood vasculature into the tumour affect the effectiveness of drug delivery [9]. The structure of a glomerular capillary wall and the glomerular permeability of macromolecules have been described in several papers and reviews [10–15]. Macromolecular clearance decreases with increasing hydrodynamic radius (R_h) and molecular weight and is influenced by polymer charge. The clearance of negatively charged macromolecules is restricted, while the clearance of positively charged macromolecules with the same molecular weight is enhanced [10]. The renal clearance of linear flexible macromolecules, such as dextran and poly(vinylpyrrolidone), is up to 10 times greater than that of proteins with equivalent hydrodynamic radii [11]. Macromolecular branching leads to decreased renal clearance and significantly prolongs blood circulation time [9,16].

* Corresponding authors. Tel.: +420 296 809 389; fax: +420 296 809 410.
E-mail addresses: subr@imc.cas.cz (V. Šubr), ulbrich@imc.cas.cz (K. Ulbrich).

0168-3659/$ – see front matter © 2012 Elsevier B.V. All rights reserved.
doi:10.1016/j.jconrel.2012.06.029

Macromolecules are typically eliminated from the body through a kidney glomerulus, which in mice or rats contains pores approximately 4 nm by 14 nm in size [17] and 8 nm in humans [18]. Macromolecules with a coil diameter smaller than glomerular pores permeate these pores and are excreted from the body in the urine [11]. The threshold for renal filtration of macromolecules with hydrodynamic radii (R_hs) below 5 nm corresponds roughly with their molecular weights, ranging from 30,000 to 50,000 g.mol^{-1}, and is influenced by their molecular architecture [9,13,19]. Noguchi demonstrated that radiolabeled poly [*N*-(2-hydroxypropyl)methacrylamide)] with different molecular weights, ranging from 4500 to 800,000 g.mol^{-1}, accumulated in tumour tissue at approximately the same rate; however, the higher molecular weight polymers accumulate in tumour tissue more than in healthy tissue and are unable to diffuse either tissue through the vasculature as rapidly as the lower molecular weight polymers [20]. The total body distribution of ^{131}I radiolabeled HPMA copolymers was monitored scintigraphically for 7 days after i.v. injection into Copenhagen rats bearing Dunning prostate carcinoma. The kinetic of tumour accumulation was dependent on copolymer molecular weight. The HPMA copolymers with MWs above the kidney threshold displayed continuous and higher accumulation than polymers with shorter chains [21,22].

Sadekar et al. compared the biodistribution of ^{125}I radiolabeled linear HPMA copolymers with branched poly(amido amine) dendrimers containing surface hydroxyl groups in ovarian-tumour-bearing mice (A2780). They found that polymer architecture affects renal and hepatic uptake, with dendrimers showing more persistent accumulation than linear HPMA copolymers. This study also showed that prolonged tumour retention may be obtained for polymers with hydrodynamic radii approximately 4 nm or higher [19].

Ideally, a drug covalently bound to a polymer conjugate should be inactive during transport through the body and should be activated (released) from the carrier at the site of its desired pharmacological effect, for example, in the solid tumour or in tumour cells either by enzymolysis or pH-controlled hydrolysis [23,24]. A broad range of HPMA copolymer (pHPMA) based conjugates have been synthesised and studied [25,26]. Further development has led to clinical trials for some of these specific drug-polymer conjugates [27–30].

Nevertheless, to properly design polymer-drug conjugates with high potential to succeed in clinical evaluation, more detailed in vivo studies are necessary. Recently, new nanomedicines based on biodegradable high-molecular weight (HMW) polymer carriers designed for treatment of solid tumours have been developed [31–33]. Among them, HMW conjugates of a star structure showed superior properties in vivo [33]. The aim of this work is to study the impact of the polymer carrier's MW and architecture on drug biodistribution and in vivo anti-cancer activity of the conjugate. For this study, HPMA copolymer conjugates bearing DOX bound by an enzymatically degradable oligopeptide GFLG spacer were selected because of their satisfactory stability in blood and efficient intracellular drug release [34,35].

2. Materials and methods

2.1. Chemicals

1-Aminopropan-2-ol, methacryloyl chloride, 2,2′-azobis (isobutyronitrile) (AIBN), *N*,*N*-dimethylformamide (DMF), *N*,*N*′-dicyclohexylcarbodiimide (DCC), 3-mercaptopropionic acid, dimethylaminopyridine (DMAP), *N*-hydroxybenzotrizole (HoBT), L-leucylglycine, glycyl-L-phenylalanine, glycylglycine, 4,5-dihydrothiazole-2-thiol, *o*-phthalaldehyde (OPA), *N*-ethyldiisopropylamine (EDPA), dimethyl sulfoxide (DMSO) and triethylamine (TEA) were purchased from Sigma-Aldrich, Czech Republic. Doxorubicin hydrochloride (DOX.HCl) was purchased from Meiji Seiko, Japan. Poly(amido amine) (PAMAM) dendrimers were purchased from Dendritic Nanotechnologies, Inc., Mount Pleasant, MI, USA.

2.2. Mice

C57BL/6 (B/6) mice were obtained from the breeding colony of the Institute of Physiology, AS CR, v.v.i. (Prague, Czech Republic). Mice were used at 8–12 weeks of age, housed in accordance with approved guidelines and provided food and water ad libitum. The Animal Welfare Committee of the Institute of Microbiology AS CR, v.v.i., approved all experiments.

2.3. Synthesis of monomers

N-(2-Hydroxypropyl)methacrylamide (HPMA) was synthesised by acylating 1-aminopropan-2-ol with methacryloyl chloride in dichloromethane in the presence of sodium carbonate as previously described [36]. M.p. 69–70 °C; elemental analysis: calc., C 58.72%, H 9.15%, N 9.78%; found, C 58.98%, H 9.18%, N 9.82%.

3-(*N*-Methacryloylglycylglycyl)thiazolidine-2-thione (Ma-GG-TT) was prepared by reacting *N*-methacryloylated glycylglycine with 4,5-dihydrothiazole-2-thiol in the presence of DCC and a catalytic amount of DMAP [37].

N-Methacryloylglycyl-DL-phenylalanyl-L-leucylglycine 4-nitrophenyl ester (Ma-GFLG-ONp) was prepared using a previously described procedure [38].

3-(*N*-Methacryloylglycyl-DL-phenylalanylleucylglycyl) thiazolidine-2-thione (Ma-GFLG-TT) was prepared according to a literature procedure [37]. Yield: 0.954 g (39%). The purity determined by HPLC was >99.2%; ^{1}H NMR [$(CD_3)_2SO$]: δ 0.84 (d, 3H, CH_3-Leu), 0.89 (d, 3H, CH_3-Leu), 1.30–1.70 (m, 3H, $CHCH_2$-Leu), 1.84 (s, 3H, CH_3), 2.70–3.10 (m, 2H, β-Phe), 3.45 (t, 2H, CH_2S), 3.50–3.75 (m, 2H, Gly), 4.15–4.35 (m, 1H, α-Leu), 4.45–4.75 (m, 5H, CH_2N, Gly, α-Phe), 5.35 (s, 1H, CH_2═), 5.69 (s, 1H, CH_2═), 7.20 (m, 5H, ArH), 8.01 (d, 1H, NH-Phe), 8.10 (m, 2H, NH-Gly), 8.25 (t, 1H, NH-Leu).

(*N*-Methacryloylglycyl-DL-phenylalanylleucylglycyl)doxorubicin (Ma–GFLG–DOX) was prepared by reacting an equivalent amount of Ma-GFLG-ONp with DOX.HCl in DMF at 4 °C as previously reported [36]. TLC: two spots at $R_f = 0.46$ and 0.4, corresponding to the D-Phe and L-Phe isomers (chloroform/methanol, 8:1); HPLC showed a single peak at 18.22 min (UV detection at 230 and 484 nm); amino acid analysis: Gly/L-Phe/D-Phe/L-Leu, 2.06:0.56:0.45:1.00.

The purities of all monomers mentioned above were examined by HPLC (Shimadzu, Japan) using a reverse-phase column (Chromolith Performance RP-18e 100–4.6 mm) with UV detection (230 nm, 305 nm or 488 nm), a water/acetonitrile gradient elution (0–100 vol.%), and a flow rate of 0.5 mL/min.

2.4. Synthesis of polymer precursors and conjugates

Multivalent copolymers of HPMA with Ma-GFLG-TT (polymers 1 and 2, Table 1) were prepared by radical solution polymerisation in DMSO at 50 or 60 °C for 6 h (AIBN, 1 or 2 wt.%; monomer concentration, 15 or 12.5 wt.%; molar ratio of HPMA: Ma-GFLG-TT, 95:5). The copolymers were isolated by precipitation in acetone/diethyl ether (1:3) and purified by re-precipitation into the same mixture. Yield: 75%.

The multivalent copolymer of HPMA with Ma-GG-TT (polymer 3, Table 1) was prepared accordingly in DMSO at 50 °C (AIBN, 1.5 wt.%; monomer concentration, 15 wt.%; molar ratio of HPMA: Ma-GG-TT, 90:10; 7 h). Yield: 72%.

Liner polymer conjugates containing amide-bonded doxorubicin (polymers 4–6 and 12) were prepared by aminolysis of TT groups of polymer precursors with DOX.HCl in DMSO in presence of TEA as previously described [36]. The drug-containing polymer was isolated by precipitation in acetone/diethyl ether, purified and fractionated by single (polymer 6) or multiple (polymer 4 and 5) gel permeation chromatography in water (Sephacryl S-300, column 1.5×60 cm). The highest and

Table 1
Characteristics of polymer precursors and conjugates.

Polymer	Spacer	M_w (g.mol^{-1})	M_w/M_n	TT content (mol%)	DOX (wt.%)	R_h (nm)
1	GFLG	24,400	1.95	3.9	–	–
2	GFLG	121,000	1.72	4.2	–	–
3	GG	87,800	1.87	9.95	–	–
4	GFLG	35,800	1.20	–	8.6	4.6
5	GFLG	96,900	1.29	–	6.8	7.8
6	GG	89,000	1.80	–	7.5	7.4
7[a]	GFLG	18,400	1.69		9.7	–
8[b]	GFLG	66,000	1.45		9.5	6.9
9[b]	GFLG	94,000	1.25		9.6	7.9
10[b]	GFLG	248,000	1.82		10.6	13.7
11[b]	AcapNHN	202,000	1.72		9.6	13.1
12	GFLG	130,000	1.50		7.4	13.8

[a] Semitelechelic polymer precursor.
[b] Star polymer conjugate.

lowest MW fractions of each polymer were removed during the separation. The final polymer conjugates (4–6) were freeze-dried.

Semitelechelic polymer precursor 7 was prepared by precipitation chain-transfer radical copolymerisation of 127.7 mg HPMA with 27.2 mg Ma–GFLG–DOX in 1.25 mL acetone using 1.5 mg AIBN as initiator and 2.43 mg 3-mercaptopropionic acid as a chain-transfer agent. The polymerisation was performed in a sealed ampoule under nitrogen at 50 °C for 23 h. The polymer was removed by filtration and purified by re-precipitation from methanol into acetone/diethyl ether (3:1). Star polymer conjugates 8 and 9 were prepared by grafting the semitelechelic polymer 7 onto the amino groups of the PAMAM dendrimer. Example of the reaction: polymer precursor 7 (33 mg) was activated by 2 mg HoBT and 3 mg DCC in 0.6 mL DMF at 15 °C. After stirring for 4 h, the polymer was added to a solution containing 1 mg PAMAM dendrimer (generation G2, 16 amino groups), the reaction was left to stir gently for another 20 h, and the star polymer conjugate was isolated by precipitation in a mixture of dry acetone/diethyl ether (1:1). After dissolution in phosphate-buffered saline, the conjugate was fractionated by single gel permeation chromatography (Sephacryl S-300, column 1.5×60 cm). The highest and lowest MW fractions were removed, and the final star polymer 9 was obtained after desalting using a Sephadex G-25 column (distilled water eluent) and freeze-drying. Star polymer conjugates 10 and 11 with DOX bound via a GFLG spacer and amide bond (10) or via a hydrazone bond (11) were synthesised accordingly by grafting PAMAM dendrimers with semitelechelic polymer precursors using a procedure described in [39]. Conjugate 11, which displays pH-controlled drug activation, was used as a control in an in vivo study in comparison to conjugates displaying enzyme-triggered drug release.

2.5. Purification and characterisation of polymers and polymer conjugates

Polymers 4–6, 8–9 and 12 were tested for free DOX content using HPLC (Shimadzu, Superose™ 6 or TSKgel G4000SW columns). The total DOX content was determined spectrophotometrically on a Helios α (Thermochrom) spectrophotometer. The molar absorption coefficient in methanol (ε_{488} = 8 100 L.mol^{-1}.cm^{-1}) was used for the calculation of drug content.

MW and polydispersity determination of the conjugates was performed on a HPLC Shimadzu system equipped with UV, an Optilab® rEX differential refractometer and MALS DAWN® 8™ (Wyatt Technology, USA) detectors. For these experiments, a 0.3 M acetate buffer (pH 6.5; 0.5 g/L NaN_3) and a Superose™ 6 column or a 20% 0.3 M acetate/80% methanol (v/v) buffer and TSKgel G4000SW column were used.

The content of thiazolidine-2-thione (TT) groups was determined spectrophotometrically on a Helios α (Thermochrom) spectrophotometer (ε_{305} = 10,700 L.mol^{-1}.cm^{-1}; methanol) [37]. The hydrodynamic radius (R_h) was determined by dynamic light scattering (DLS) using an aqueous solution of polymer conjugates and a scattering angle of 173° on a Nano-ZS, Model ZEN3600 (Malvern, UK) zetasizer.

The content of end carboxylic groups in semitelechelic polymer precursor 7 was determined by titration with 0.05 N NaOH using an automatic titrator TIM900 (Radiometer). From the concentration of the end carboxylic groups, the average molecular weight ($M_{n,COOH}$) of semitelechelic polymer precursor 7 was calculated.

2.6. Blood clearance and determination of DOX content in the urine, liver and tumour tissues

C57BL/6 (B/6) male mice were inoculated subcutaneously with 1×10^5 EL4 lymphoma cells. When the tumour reached a volume of 50 − 75 mm^3, the mice were injected intravenously (i.v.) with either DOX.HCl (5 mg/kg) or conjugates 4–6 or 8–9 (15 mg DOX eq./kg represents an equitoxic dose). Blood, urine, liver and tumour tissue samples were taken at the following times after injection: 1, 3, 6, 9, 12, 24, 30, 36, 48, and 72 h for blood and urine (5 mice per group) and 6, 12, 24, 48, and 72 h for the liver and tumour tissues (3 mice per group). The blood samples were collected in heparinised tubes, while the liver and tumour samples were excised, weighed and homogenised. The samples were tested for their total DOX content (i.e., the sum of free and polymer-bound DOX) and molecular weights and polydispersities of the polymer conjugates eliminated from the body in urine.

The total DOX content in the samples was determined after quantitative acid hydrolysis (1 M HCl, 1 h at 50 °C) of the respective samples. The doxorubicinone, formed from free and polymer-bound doxorubicin after hydrolysis, was extracted with chloroform, and the organic phase was evaporated to dryness. The remaining solid was completely dissolved in methanol and analysed using a gradient-based HPLC Shimadzu system equipped with a Shimadzu RF-10Axl fluorescence detector (λ_{exc} = 488 nm, λ_{em} = 560 nm) [40]. Calibration was performed by injection of exact amounts of free DOX.HCl into the blood, urine and tumour tissue obtained from untreated animals followed by analysis (samples were homogenised, hydrolysed and extracted) as described above. The molecular weight, polydispersity and amount of polymer conjugate in each urine sample were determined on HPLC Shimadzu system equipped with a TSKgel G4000SW column (dn/dc = 0.170 mL.g^{-1}) and LS, RI and fluorescence detectors after desalting the samples on PD10 columns (700 μL urine was injected onto PD-10 column, eluent distilled water) and freeze-drying of eluted polymer fraction. Extraction of urine samples did not show presence of significant amount of free DOX.

2.7. In vivo evaluation of anti-cancer activity

B/6 males were subcutaneously (s.c.) transplanted with 1×10^5 EL4 T cell lymphoma cells on the right flank (day 0). The mice that developed palpable tumours reaching 50–75 mm^3 were injected i.v. with 200 μL of polymer conjugates or free drug PBS solutions (for dosage, see Results and discussion). The doses referred to hereafter are expressed as mg of DOX equivalent per kg. Control mice were transplanted with tumour cells and left untreated. The animals (8 mice per group) were observed for signs of tumour progression and acute toxicity. Tumour size, body weight, survival time and number of long-term survivors were determined. Those surviving at least 60 days without any signs of tumour are considered long-term survivors (LTS).

2.8. Statistics

The statistical significance ($P<0.05$) of the differences between volumes of tumours in the various groups was assessed by applying a two-sided Student's *t*-test. For each approach, three independent experiments were conducted and differences between exposed and

control animals with an error probability of $P<0.05$ were considered to be statistically significant.

3. Results and discussion

Recently, increased attention has been paid to the development of new HMW polymer drug carrier systems that will enable enhanced tumour accumulation via the EPR effect [33,41]. We have previously demonstrated the remarkable in vivo efficiencies of HMW HPMA copolymer-DOX conjugates designed for solid tumour treatment. Specifically, we found that increasing the molecular weight of such polymer carriers above the limit of renal filtration led to decreased elimination of the polymers from circulation by kidney clearance, which resulted in prolonged blood circulation half-times in the organism and enhanced accumulation of the drug in solid tumours due to the EPR effect. To avoid undesirable long-term accumulation of the HMW polymer carrier in the body, such polymer constructs must contain biodegradable spacers susceptible to body-related biodegradation, namely hydrolysis or reduction [33,42]. Polymer carriers based on HPMA may either be eliminated from the organism by the quick process of renal filtration or by slower processes via the liver and bile.

This paper is focused on the synthesis of HMW polymer-DOX conjugates differing in molecular weight, polydispersity and molecular architecture and the study of their physicochemical and preliminary biological properties, specifically tumour and liver accumulation, blood clearance and urine elimination. Four of the synthesised conjugates were linear polymers (see Fig. 1) that differed in polydispersity and molecular weight, and their molecular weights were either below or above the generally accepted kidney elimination threshold (~40,000 $g.mol^{-1}$). The other synthesised polymer-DOX conjugates were prepared by grafting semitelechelic HPMA copolymers onto a PAMAM dendrimer core to form HMW star structures (see Fig. 2). Except for conjugate 11, all synthesised polymer conjugates contained a GFLG spacer and an amide bond-bound DOX.

The primary goal of this study was to demonstrate that molecular architecture, polydispersity and molecular weight strongly influence tumour accumulation, blood clearance and urine elimination of polymer-DOX conjugates with direct impact on their anti-cancer activities. Moreover, we aimed to show that water-soluble linear polymers, even with molecular weights above the generally accepted renal threshold for HPMA polymers (~40,000 $g.mol^{-1}$), could also be removed by renal filtration.

3.1. Synthesis of polymer precursors and conjugates

Multivalent polymer precursors 1 to 3 with molecular weights ranging from 25,000 to 120,000 $g.mol^{-1}$ and containing reactive TT groups susceptible to aminolysis were prepared by radical solution copolymerisation in DMSO [37]. These precursors enabled synthesis of linear polymer-DOX conjugates 4–6 and 12 (Table 1) by simple aminolytic reaction with DOX.HCl in DMSO containing TEA as a base. Polymer conjugates 4 and 5 were subsequently fractionated by gel chromatography to obtain polymer-DOX conjugates with low polydispersities and with MWs below (conjugate 4) and above (conjugates 5 and 12) the renal threshold [43].

Semitelechelic polymer 7 (Table 1) was prepared by radical solution copolymerisation of HPMA with Ma–GFLG–DOX initiated with AIBN in the presence of 3-mercaptopropionic acid as the chain-transfer agent. Use of this method enabled preparation of a semitelechelic polymer-DOX precursor with a functionality (or number of end chain carboxylic groups per polymer chain) close to 1 ($M_n/M_{n,COOH}$ ~ 0.97).

Star polymer conjugates 8 and 9, which differ only in molecular weight, were prepared by grafting semitelechelic polymer 7 onto a PAMAM dendrimer (generation 2) containing 16 amino groups using a DCC coupling method. The products of the grafting reaction were water-soluble HMW polymers with star structures. Polymer conjugates 8 and 9 were fractionated by gel chromatography to obtain polymer conjugates with low polydispersities, comparable to the polydispersities of polymer conjugates 4 and 5. The molecular

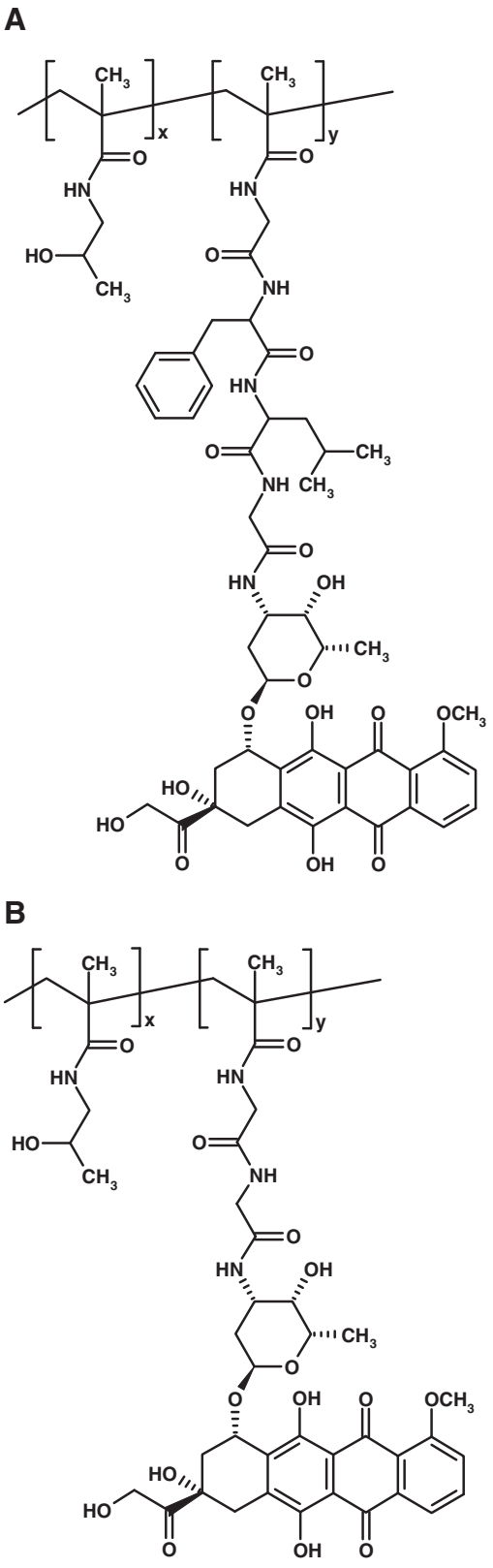

Fig. 1. Structures of polymer-DOX conjugates: (A) conjugates 4 or 5 containing amide-bonded DOX attached to a GFLG spacer, which is degradable by lysosomal enzymes, (B) conjugate 6 containing amide-bonded DOX attached to a nondegradable GG spacer.

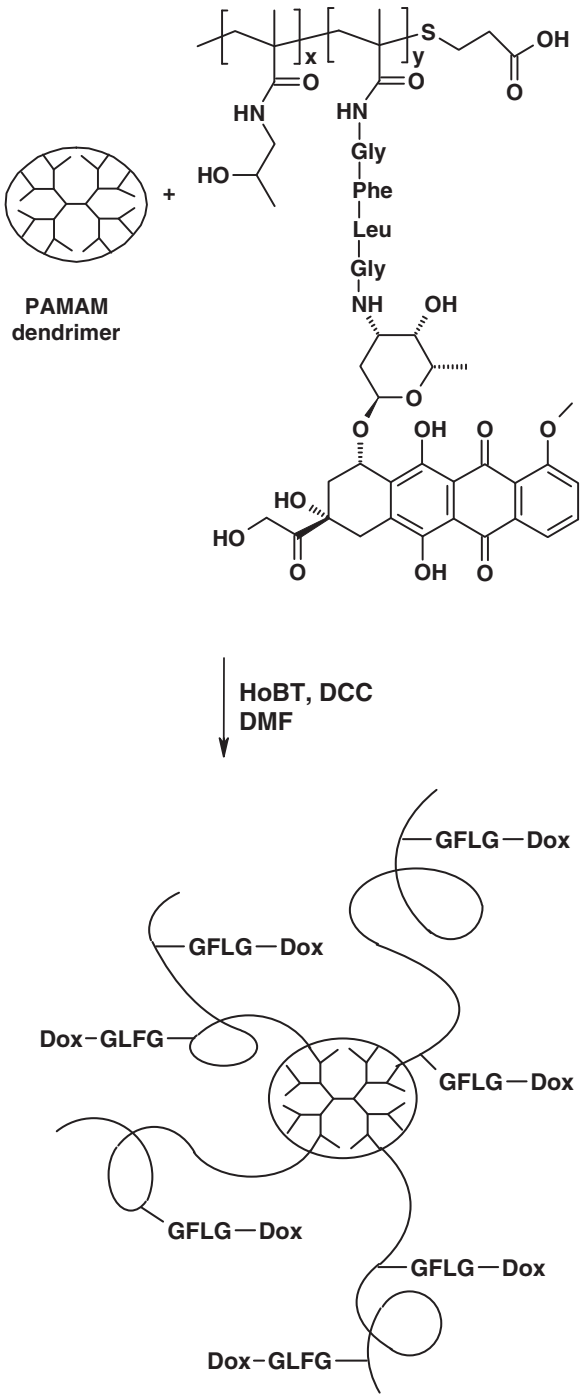

Fig. 2. Schematic description of the synthesis of star polymer-DOX conjugates 8 and 9.

weights of the resulting star polymers reflected that, on average, four semitelechelic polymers were attached to the dendrimer core in star polymer conjugate 8, and six polymer chains were attached to polymer conjugate 9.

The hydrodynamic radii (R_h) of the linear and star polymer-DOX conjugate coils in aqueous solution increased from ~5 nm to almost 14 nm depending on molecular weight. As expected, the size of HMW linear conjugate 12 was slightly higher than it would correspond with the size of branched star conjugates of the same molecular weights.

As previously described, DOX release from HPMA-based polymer conjugates containing DOX attached via oligopeptide spacers is controlled by the structure of the oligopeptide spacer and the concentration of the respective enzyme responsible for its cleavage [23,33,44]. No significant DOX release from polymer conjugates containing a diglycine spacer was observed during incubation in human serum [34] or lysosomal enzymes. Such a spacer is considered nondegradable (here, conjugate 6) because the conjugate does not release drug, and thus, this spacer was used in this study. Conversely, conjugates containing a GFLG spacer release DOX in the presence of cathepsin B (5×10^{-7} M) or lysosomal enzymes (tritosomes), with rates being three times higher for linear polymers than for polymers with the HMW star structure [33]. Almost no release was observed in serum. For this biodistribution study, we used conjugates containing GFLG spacers rather than the recently developed conjugates with DOX bound via a pH-sensitive hydrazone bond [33] even though these conjugates are highly effective in vivo; because of their low stability in circulating blood, they are not as suitable for a biodistribution study.

3.2. Tumour and liver accumulation, blood clearance and excretion in urine studies

Tissue accumulation, blood clearance, and excretion in urine of doxorubicin injected in the form of water-soluble polymer-DOX conjugates differing in molecular weights, polydispersities and molecular architecture were studied in B6 mice bearing EL4 T-cell lymphoma. Our aim was to select the polymer-drug carrier with the most suitable structure for designing nanomedicines intended for the treatment of solid tumours.

3.2.1. Tumour and liver accumulation

Biodistribution study of HMW star conjugates with M_w above 200,000 g.mol^{-1} showed efficient tumour accumulation [39,45]. One of the aims of this study consisted in comparison of behaviour of linear and star conjugates with lower M_w ($\leq$100,000 g.mol^{-1}) and verification of ability of the star conjugates to be accumulated in tumours with similar efficiency as their HMW analogues. Tumour accumulation of free doxorubicin (DOX.HCl) and its polymer conjugates 4–6 and 8–9 are compared in Fig. 3. All polymer conjugates show significantly higher tumour accumulation in comparison to DOX.HCl; however, HMW conjugates 5, 6, 8 and 9, with MWs higher than the kidney threshold, displayed considerable tumour accumulation in comparison to polymer conjugate 4, which has a MW below this limit. Interestingly, no significant effect of conjugate polydispersity (compare conjugates 5 and 6) on tumour accumulation was observed. Therefore, prolonged tumour retention of the polymer conjugates can only be attributed to a defective or nonexistent lymphatic system [6,46]. The highest amount of accumulated DOX was achieved after administration of star polymer conjugate 9, while the

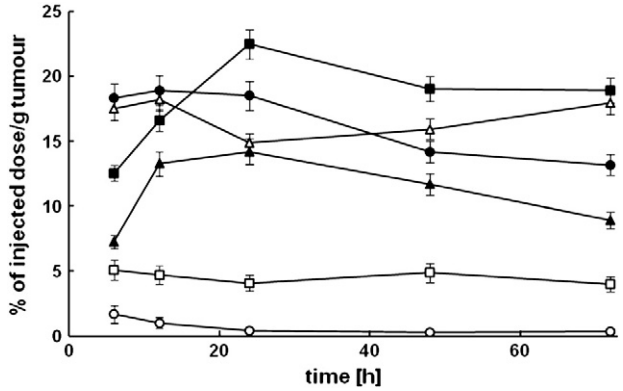

Fig. 3. Tumour accumulations in three C57BL/6 mice bearing EL4 lymphoma after i.v. injection of DOX.HCl (5 mg/kg) or conjugates 4–6 or 8–9 (15 mg DOX eq./kg, an equitoxic dose): (○ —) DOX·HCl, (□ —) conjugate 4, (Δ —) conjugate 5, (●—) conjugate 6, (▲ —) conjugate 8, and (■ —) conjugate 9.

accumulation of DOX from linear conjugates 5 and 6 with comparable molecular weights was lower. The time needed to reach maximum tumour DOX accumulation exceeded 10 h and did not depend on the architecture of polymer conjugates. Star polymer conjugates 8 and 9 seemed to accumulate in the tumour more slowly than linear conjugates. It also seems that the molecular weight of star conjugates, once exceeding renal threshold, do not significantly influence tumour accumulation (compare with Ref. [45]). In all cases, the drug remains accumulated in the tumour for a long period of time.

Liver accumulations of DOX.HCl and polymer conjugates 4–6 and 8–9 (Fig. 4) showed that the amount of polymer conjugates 4–6 and 8–9 in the liver exhibits a similar dependency on molecular weight as previously shown for tumour accumulation. In contrast to tumour accumulation, however, the concentration of polymer conjugates 4–6 and 8–9 in the liver increased during the first 24 h and decreased during the following 48 h due to an efficient lymphatic and, perhaps, hepatobiliary elimination system, which confirms previously published conclusions [6,46].

3.2.2. Blood clearance

Blood clearance of linear conjugates 4–6 and star conjugates 8 and 9 was compared to that of free DOX.HCl (Fig. 5). The low-molecular-weight DOX.HCl cleared from the bloodstream very rapidly, being significantly faster than its polymer conjugates. As expected, polymer architecture, hydrodynamic radius (R_h) and weight average molecular weight (M_w) of each conjugate significantly influenced the rate of elimination from blood circulation. Blood clearance of linear polymer conjugates 5 and 6 and star polymer conjugates 8 and 9, with molecular weights above the kidney elimination threshold, were much slower than that of linear conjugate 4, which could be more easily removed from circulation by glomerular filtration [21,22]. Interestingly, these results agree with the cumulative amount of conjugates 4–6 and 8–9 found in urine fractions collected within a 72 h period after the administration of the conjugates (Fig. 6).

3.2.3. Excretion of the polymers in urine

The amount of polymer conjugate eliminated through the kidney in urine fractions was determined by two methods. The first method calculated the amount of polymer in urine fractions from the content of DOX without characterising the excreted polymer. The second method (HPLC) enabled the calculation of the amount of polymer-DOX in the urine and molecular characterisation of the conjugate. The calculated amounts of polymer-DOX conjugate in urine fractions, determined by both independent methods, were in good agreement (Table 2). It is understandable because DOX release from the conjugates in blood circulation and urine is negligible and practically all DOX is in its polymeric form (results not shown).

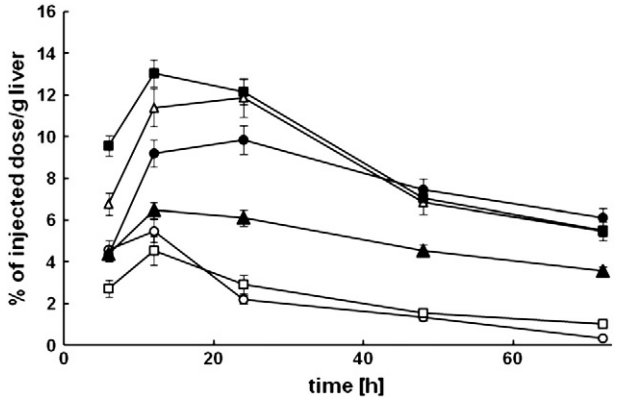

Fig. 4. Liver accumulations in three C57BL/6 mice bearing EL4 lymphoma after i.v. injection of DOX.HCl (5 mg/kg) or conjugates 4–6 or 8–9 (15 mg DOX eq./kg, an equitoxic dose): (○ —) DOX·HCl, (□ —) conjugate 4, (Δ —) conjugate 5, and (●—) conjugate 6, (▲ —) conjugate 8, and (■ —) conjugate 9.

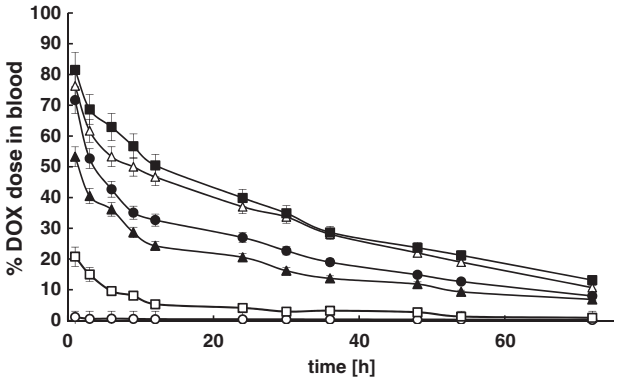

Fig. 5. Blood clearance in five C57BL/6 mice bearing EL4 lymphoma after i.v. injection of DOX.HCl (5 mg/kg) or conjugates 4–6 or 8–9 (15 mg DOX eq./kg, an equitoxic dose): (○ —) DOX·HCl, (□ —) conjugate 4, (Δ —) conjugate 5, (●—) conjugate 6, (▲ —) conjugate 8, and (■ —) conjugate 9.

Characteristics of the polymers (conjugates 4–6, 8, and 9) eliminated from the body through kidney clearance collected in urine within 72 h or 96 h after i.v. administration are summarised in Tables 2 and 3. The results show that each polymer is not eliminated as a whole but rather as polymer fractions with very narrow molecular weight distribution; the polymers with the lowest molecular weights were excreted first, followed by the higher molecular weight fractions (Table 2). This phenomenon was observed for both the linear and star polymer conjugates. After 72 h, the molecular weight of the polymer eliminated by renal filtration reached almost 70,000 g.mol^{-1} for linear polymer conjugates 4–6, which can be considered the threshold limit for elimination of linear HPMA conjugates through the kidney.

In contrast, for star conjugates 8 and 9, the threshold limit was approximately 50,000 g.mol^{-1} (see Table 3), which is in agreement with the literature [47]. The differences observed in excretion limits can be attributed to a different mechanism of polymer passage through the kidney glomerulus. Filtration of the highly branched star polymers are primarily controlled by the diameter of the relatively rigid polymer coil in solution, while the limit for linear molecules may be higher; transport of even larger polymer chains can be improved by possible worm-like movement of such molecules through the pores of glomerulus. Of course, such transport is slower than simple filtration and comes into effect in later stages of polymer elimination (36–96 h).

It is also clear that the amount of excreted polymer depends on the polydispersity of the original conjugate; more disperse conjugates contain a higher portion of shorter polymer chains that can be filtered

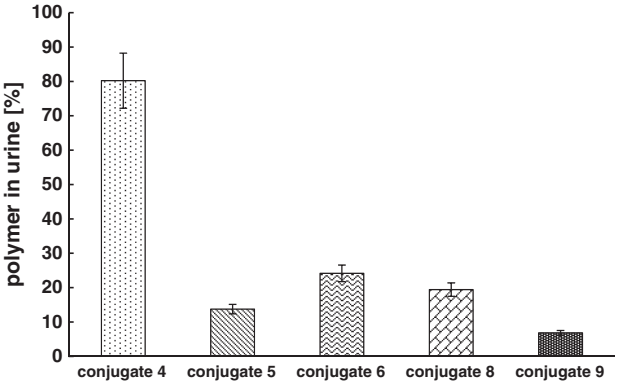

Fig. 6. Cumulative urine eliminations of linear conjugates 4–6 and star conjugates 8–9 from C57BL/6 mice (5 in group) bearing EL4 lymphoma (i.v. injection; 72 h). 15 mg DOX eq./kg was injected (i.v.).

Table 2
Characteristics of linear polymer conjugates isolated from urine.

	Conjugate 4			Conjugate 5			Conjugate 6		
Time (h)	M_w (g.mol^{-1})	M_w/M_n	% ([a]/[b])	M_w (g.mol^{-1})	M_w/M_n	% ([a]/[b])	M_w (g.mol^{-1})	M_w/M_n	%
1	19,100	1.05	38.7/35.7	29,800	1.04	4.3/4.8	23,950	1.07	8.8/8.3
3	22,000	1.06	24.7/26.1	33,000	1.06	2.8/3.6	26,700	1.07	6.8/6.4
6	28,000	1.05	3.1/4.1	39,000	1.05	1.2/1.7	31,000	1.05	1.5/1.2
9	28,800	1.07	2.6/3.6	41,500	1.08	1.0/1.3	32,300	1.06	0.5/0.6
12	33,000	1.20	3.2/4.1	50,500	1.11	1.0/1.0	35,100	1.05	1.4/1.4
24	39,100	1.10	3.9/3.2	51,000	1.17	1.5/0.9	36,000	1.07	1.4/1.2
30	41,500	1.12	1.1/0.4	62,300	1.14	0.9/0.3	40,200	1.14	0.5/0.3
36	48,000	1.10	0.8/0.3	66,000	1.16	0.5/0.2	49,200	1.25	0.1/0.3
48	53,000	1.32	0.8/0.3	68,800	1.19	0.5/0.2	53,200	1.26	0.8/0.4
72	68,000	1.20	1.4/0.4	69,000	1.22	0.1/0.4	69,100	1.32	0.1/0.3

[a] Percent of polymer in the urine sample determined by the DOX content.
[b] Percent of polymer in the urine sample determined by GPC via dn/dc.

in an initial phase of polymer excretion (compare conjugates 5 and 6, Table 3).

The cumulative amounts of polymer conjugates 4–6, 8, and 9 eliminated by renal filtration are shown in Fig. 6. After 72 h, 80% of polymer conjugate 4, with the lowest molecular weight, was eliminated by renal filtration; conjugates 5 and 6, with higher molecular weights, exhibited lower cumulative amounts eliminated by the kidneys, with the more polydisperse conjugate 6 cleared from the blood faster (Fig. 5) and excreted in the urine to a larger extent (25%) than monodisperse conjugate 5 (15%). The cumulative amounts of HMW star polymer conjugates 8 and 9 eliminated by renal filtration were lower than those amounts for conjugates 4–6 of similar molecular weights, demonstrating the influences of a more rigid molecular architecture. Therefore, it is clear that complete elimination of the HMW linear and star polymer conjugates intended for in vivo treatment can only be achieved by designing polymer carrier systems containing biodegradable linkages enabling polymer carrier fragmentation to sequences with molecular weights sufficiently below kidney threshold [33,45].

3.3. In vivo anti-cancer activity

Anti-tumour activity of linear and star HPMA copolymer-DOX conjugates was tested in C57BL/6 (B/6) mice with s.c. implanted murine syngeneic tumour model EL4 T-cell lymphoma (1×10^5). The effect of HMW conjugates with R_h ~13 nm and conjugates with lower M_w (conjugate 4) were evaluated. eq./kg.

The mice (8 per group) were treated i.v. on day 8 after cell transplantation with a single dose of the conjugates, either 15, 10 or 5 mg DOX No weight loss or other signs of acute toxicity (data not shown) were observed after conjugate injection. In most cases, inhibition or even regression of tumour growth was observed. Overall survival of mice after treatment with star (Fig. 7) or linear (Fig. 8) HPMA copolymer-DOX conjugates depended on the dose and molecular weight of the conjugate. Treatment of mice with 15 mg DOX eq./kg of the HMW star polymer conjugate (Fig. 7) with DOX bound via a GFLG spacer (conjugate 10) or with the similar conjugate bearing DOX bound via pH-sensitive hydrazone bond (conjugate 11) resulted in complete tumour regression of all animals, as 100% of animals were considered long-term surviving (LTS). A decrease in the dose to 10 mg DOX eq./kg resulted in lower efficacy of treatment, resulting in 75% LTS for conjugate 11 (hydrazone bond) and 63% for conjugate 10 (amide bond). A further decrease in the dose to 5 mg DOX eq./kg produced only 37% LTS in case of conjugate 11 and no LTS for conjugate 10. Conjugates containing the GFLG spacer and amide bond are somewhat less effective than their corresponding conjugates containing the pH-sensitive hydrazone bond, but this difference is relatively small. Animals treated with 10 mg DOX eq./kg of a HMW linear conjugate 12 (Fig. 8) exhibited similar survival (75% LTS) as respective star conjugate, while treatment with conjugate 4 (M_w 36 000 g.mol^{-1}) was much less effective, thus indicating the importance of the EPR effect on final anti-tumour activity. The survival data shown above are in good agreement with tumour growth/regression data shown as supplementary in Figs. 9 and 10 (see supplement). The results shown in Figs. 7 and 8 indicate that anti-tumour activity of the conjugates depends more on the size of their coil in solution (R_h of HMW conjugates ~13–14 nm, R_h of conjugate 4–4.5) than on molecular weight and detailed polymer structure.

The results of our evaluation of anti-cancer activity of HPMA copolymer conjugates show that the HMW star conjugates with the lowest blood clearance rate and the highest tumour accumulation exhibit the highest anti-tumour activity in vivo, with complete tumour regression of animals at 15 mg DOX eq./kg, and this activity is

Table 3
Characteristics of star polymer conjugates isolated from urine.

Time (h)	Conjugate 8		% ([a])	Conjugate 9		% ([a])
	M_w (g.mol^{-1})	M_w/M_n		M_w (g.mol^{-1})	M_w/M_n	
1	22,650	1.06	3.9	43,000	1.14	1.8
3	25,600	1.08	3.5	44,800	1.07	0.8
6	33,650	1.03	2.3	47,000	1.04	0.6
12	38,100	1.02	1.8	47,000	1.08	0.8
24	38,000	1.03	1.8	48,000	1.05	0.8
48	44,000	1.12	1.6	50,300	1.06	0.8
72	49,000	1.05	1.6	52,000	1.08	0.6
96	51,200	1.04	2.0	53,300	1.15	0.3

[a] Percent of polymer in the urine sample determined by the DOX content.

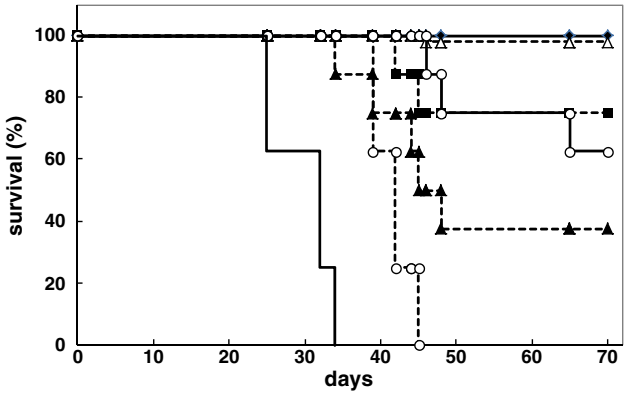

Fig. 7. Survival of EL4 T-cell lymphoma-bearing B/6 mice treated with star polymer-DOX conjugates. B/6 mice were transplanted s.c. with 1×10^5 EL4 T-cells and treated with (○- - -) DOX.HCl, two doses, 5 mg DOX/kg each; (♦ —) conjugate 11, 1×15 mg DOX eq./kg; (■—) conjugate 11, 1×10 mg DOX eq./kg; (▲- - -) conjugate 11, 1×5 mg DOX eq./kg; (Δ - - -) conjugate 10, 1×15 mg DOX eq./kg; (○—) conjugate 10, 1×10 mg DOX eq./kg; using i.v. drug administration on day 8. Control mice (—) were left untreated.

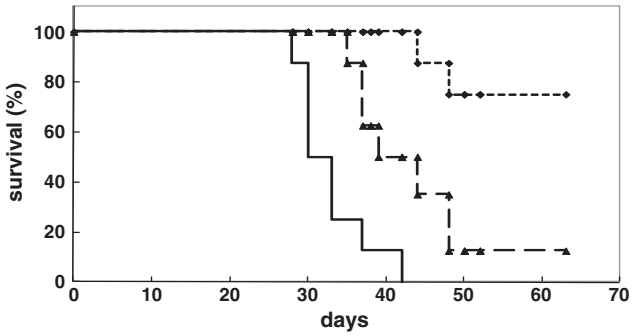

Fig. 8. Survival of EL4 T-cell lymphoma-bearing B/6 mice treated with linear polymer-DOX conjugates. B/6 mice were transplanted s.c. with 1×10^5 EL4 T-cells and treated with (♦- - -) conjugate 12, 1×10 mg DOX eq./kg or (▲- - -) conjugate 4, 1×10 mg DOX eq./kg using i.v. drug administration on day 8. Control mice (—) were left untreated.

practically independent on mode of drug attachment (e.g., enzymatically or hydrolytically cleavable hydrazone spacers). This finding is quite surprising because all experiments previously performed with HPMA copolymer-doxorubicin conjugates with molecular weights below the renal threshold have displayed much higher conjugate activity when DOX was bound via hydrazone bond compared to conjugates containing a GFLG spacer; furthermore, such a dramatic anti-cancer effect in the case of GFLG spacer-containing conjugates was unexpected (this was why conjugate 10 with M_w 248 kDa was selected for in vivo evaluation to achieve higher activity than was expected from conjugate 9 (94 kDa).

4. Conclusions

The present study describes the synthesis, physicochemical characterisation and determination of biological properties, namely blood clearance, kidney elimination, tumour and liver accumulation and survival of mice bearing EL 4 T-cell lymphoma after i.v. injection of HPMA copolymer-DOX conjugates. The conjugates differed in molecular weights, polydispersities and molecular architecture.

The biological properties of linear polymer-DOX conjugates with different molecular weights and polydispersities were compared to the properties of dendrimer core-based star polymer-DOX conjugates with relatively rigid structures.

The molecular weights of the linear polymer-DOX conjugates excreted in urine of mice by renal filtration were up to 70,000 $g.mol^{-1}$, while the highest molecular weight of the star conjugates excreted in urine was ~50,000 $g.mol^{-1}$. The amount of polymer-DOX conjugate eliminated by renal filtration decreased with increasing molecular weight, and linear conjugates with comparable molecular weights to the star conjugates were eliminated more quickly. Polymers were not excreted in urine as the whole polymer fraction with molecular weights below 50,000 $g.mol^{-1}$ but were rather excreted as narrow polymer fractions with molecular weights gradually increasing with time following injection (excreted urine volume). Finally, polymer-DOX conjugates with higher molecular weights exhibited longer blood circulation times and higher tumour accumulations, which resulted in significantly improved anti-tumour activities of the HMW conjugates in vivo, independent of drug attachment form.

Acknowledgements

This work was supported by the grant agency of the Academy of Sciences of the Czech Republic (grant no. IAAX00500803) and the grant agency of the Czech Republic (grant no. P301/11/0325).

Appendix A. Supplementary data

Supplementary data to this article can be found online at http://dx.doi.org/10.1016/j.jconrel.2012.06.029.

References

[1] G. Pasut, M. Sergi, F.M. Veronese, Anti-cancer PEG-enzymes: 30 years old, but still a current approach, Adv. Drug Deliv. Rev. 60 (2008) 69–78.
[2] R. Duncan, Polymer conjugates as anticancer nanomedicines, Nat. Rev. Cancer 6 (2006) 688–701.
[3] J. Kopeček, Biomaterials and drug delivery: past, present, and future, Mol. Pharm. 7 (2010) 922–925.
[4] B. Říhová, L. Kovář, M. Kovář, O. Hovorka, Cytotoxicity and immunostimulation: double attack on cancer cells with polymeric therapeutics, Trends Biotechnol. 27 (2009) 11–17.
[5] B. Říhová, M. Kovář, Immunogenicity and immunomodulatory properties of HPMA-based polymers, Adv. Drug Deliv. Rev. 62 (2010) 184–191.
[6] Y. Matsumura, H. Maeda, A new concept for macromolecular therapeutics in cancer-chemotherapy — mechanism of tumoritropic accumulation of proteins and the antitumor agent Smancs, Cancer Res. 46 (1986) 6387–6392.
[7] H. Maeda, K. Greish, J. Fang, The EPR effect and polymeric drugs: a paradigm shift for cancer chemotherapy in the 21st century, In: in: R. Satchi-Fainaro, R. Duncan (Eds.), Advances in Polymer Science, Springer, Berlin/Heidelberg, 2006, pp. 103–121.
[8] H. Maeda, Tumor-selective delivery of macromolecular drugs via the EPR effect: background and future prospects, Bioconjug. Chem. 21 (2010) 797–802.
[9] M.E. Fox, F.C. Szoka, J.M.J. Frechet, Soluble polymer carriers for the treatment of cancer: the importance of molecular architecture, Acc. Chem. Res. 42 (2009) 1141–1151.
[10] H.G. Rennke, M.A. Venkatachalam, Glomerular-permeability of macromolecules — effect of molecular-configuration on the fractional clearance of uncharged dextran and neutral horseradish-peroxidase in the rat, J. Clin. Invest. 63 (1979) 713–717.
[11] M.A. Venkatachalam, H.G. Rennke, Structural and molecular-basis of glomerular-filtration, Circ. Res. 43 (1978) 337–347.
[12] W.M. Deen, M.J. Lazzara, B.D. Myers, Structural determinants of glomerular permeability, Am. J. Physiol. Renal Physiol. 281 (2001) F579–F596.
[13] J. Tencer, I.M. Frick, B.W. Oquist, P. Alm, B. Rippe, Size-selectivity of the glomerular barrier to high molecular weight proteins: upper size limitations of shunt pathways, Kidney Int. 53 (1998) 709–715.
[14] D. Asgeirsson, D. Venturoli, E. Fries, B. Rippe, C. Rippe, Glomerular sieving of three neutral polysaccharides, polyethylene oxide and bikunin in rat. Effects of molecular size and conformation, Acta Physiol. 191 (2007) 237–246.
[15] D. Asgeirsson, J. Axelsson, C. Rippe, B. Rippe, Similarity of permeabilities for Ficoll, pullulan, charge-modified albumin and native albumin across the rat peritoneal membrane, Acta Physiol. 196 (2009) 427–433.
[16] N. Nasongkla, B. Chen, N. Macaraeg, M.E. Fox, J.M.J. Frechet, F.C. Szoka, Dependence of pharmacokinetics and biodistribution on polymer architecture: effect of cyclic versus linear polymers, J. Am. Chem. Soc. 131 (2009) 3842–3843.
[17] R. Rodewald, M.J. Karnovsky, Porous substructure of glomerular slit diaphragm in rat and mouse, J. Cell Biol. 60 (1974) 423–433.
[18] A.C. Guyton, J.E. Hall, Textbook of Medicinal Physiology, In: Elsevier Saunders, Philadelphia, 2006, pp. 316–317.
[19] S. Sadekar, A. Ray, M. Janat-Amsbury, C.M. Peterson, H. Ghandehari, Comparative biodistribution of PAMAM dendrimers and HPMA copolymers in ovarian-tumor-bearing mice, Biomacromolecules 12 (2011) 88–96.
[20] Y. Noguchi, J. Wu, R. Duncan, J. Strohalm, K. Ulbrich, T. Akaike, H. Maeda, Early phase tumor accumulation of macromolecules: a great difference in clearance rate between tumor and normal tissues, Jpn. J. Cancer Res. 89 (1998) 307–314.
[21] M. Kissel, P. Peschke, V. Šubr, K. Ulbrich, J. Schuhmacher, J. Debus, E. Friedrich, Synthetic macromolecular drug carriers: biodistribution of poly[*N*-(2-hydroxypropyl)methacrylamide] copolymers and their accumulation in solid rat tumors, PDA J. Pharm. Sci. Technol. 55 (2001) 191–201.
[22] T. Lammers, R. Kuhnlein, M. Kissel, V. Šubr, T. Etrych, R. Pola, M. Pechar, K. Ulbrich, G. Storm, P. Huber, P. Peschke, Effect of physicochemical modification on the biodistribution and tumor accumulation of HPMA copolymers, J. Control. Release 110 (2005) 103–118.
[23] V. Šubr, J. Strohalm, K. Ulbrich, R. Duncan, I.C. Hume, Polymers containing enzymatically degradable bonds, XII. Effect of spacer structure on the rate of release of daunomycin and adriamycin from poly-[2-(hydroxypropyl)methacrylamide] drug carriers in vitro and antitumour activity measured in vivo, J. Control. Release 18 (1992) 123–132.
[24] T. Etrych, M. Jelínková, B. Říhová, K. Ulbrich, New HPMA copolymers containing doxorubicin bound via pH-sensitive linkage: synthesis and preliminary in vitro and in vivo biological properties, J. Control. Release 73 (2001) 89–102.
[25] R. Duncan, *N*-(2-Hydroxypropyl)methacrylamide copolymer conjugates, In: in: G.S. Kwon (Ed.), Drugs and the Pharmaceutical Sciences, Polymeric Drug Delivery Systems, vol. 148, Taylor & Francis, Boca Raton, 2005, pp. 1–92.
[26] K. Ulbrich, V. Šubr, Synthetic polymer-drug conjugates for human therapy, In: in: M.M. Amiji, V.P. Torchilin (Eds.), Handbook of Materials for Nanomedicine, vol.1, Pan Stanford Publishing, 2010, pp. 5–79.
[27] R. Duncan, M.J. Vicent, Do HPMA copolymer conjugates have a future as clinically useful nanomedicines? A critical overview of current status and future opportunities, Adv. Drug Deliv. Rev. 62 (2010) 272–282.

[28] L.W. Seymour, D.R. Ferry, D.J. Kerr, D. Rea, M. Whitlock, R. Poyner, Ch. Boivin, S. Hesslewood, Ch. Twelves, R. Blackie, A. Schatzlein, D. Jodrell, D. Bissett, H. Calvert, M. Lind, A. Robbins, S. Burtles, R. Duncan, J. Cassidy, Phase II studies of polymer-doxorubicin (PK1, FCE28068) in the treatment of breast, lung and colorectal cancer, Int. J. Oncol. 34 (2009) 1629–1636.
[29] B. Říhová, K. Kubáčková, Clinical implications of *N*-(2-hydroxypropyl)methacrylamide copolymers, Curr. Pharm. Biotechnol. 4 (2003) 311–322.
[30] B. Říhová, Clinical experience with anthracycline antibiotics-HPMA copolymer-human immunoglobulin conjugates, Adv. Drug Deliv. Rev. 61 (2009) 1149–1158.
[31] T. Etrych, P. Chytil, T. Mrkvan, M. Šírová, B. Říhová, K. Ulbrich, Conjugates of doxorubicin with graft HPMA copolymers for passive tumor targeting, J. Control. Release 132 (2008) 184–192.
[32] P. Chytil, T. Etrych, Č. Koňák, M. Šírová, T. Mrkvan, J. Bouček, B. Říhová, K. Ulbrich, New HPMA copolymer-based drug carriers with covalently bound hydrophobic substituents for solid tumour targeting, J. Control. Release 127 (2008) 121–130.
[33] T. Etrych, J. Strohalm, P. Chytil, P. Černoch, L. Starovoytova, M. Pechar, K. Ulbrich, Biodegradable star HPMA polymer conjugates of doxorubicin for passive tumor targeting, Eur. J. Pharm. Sci. 42 (2011) 527–539.
[34] P. Rejmanová, J. Kopeček, R. Duncan, J.B. Lloyd, Stability in rat plasma and serum of lysosomally degradable oligopeptide sequences in *N*-(2-hydroxypropyl)methacrylamide copolymers, Biomaterials 6 (1985) 45–48.
[35] R. Duncan, P. Kopečková-Rejmanová, J. Strohalm, I.C. Hume, H.C. Cable, J. Pohl, J.B. Lloyd, J. Kopeček, Anticancer agents coupled to N-(2-hydroxypropyl)methacrylamide copolymers. 1. Evaluation of daunomycin and puromycin conjugates in vitro, Br. J. Cancer 55 (1987) 165–174.
[36] K. Ulbrich, V. Šubr, J. Strohalm, D. Plocová, M. Jelínková, B. Říhová, Polymeric drugs based on conjugates of synthetic and natural macromolecules I. Synthesis and physico-chemical characterisation, J. Control. Release 64 (2000) 63–79.
[37] V. Šubr, K. Ulbrich, Synthesis and properties of new *N*-(2-hydroxypropyl)methacrylamide copolymers containing thiazolidine-2-thione reactive groups, React. Funct. Polym. 66 (2006) 1525–1538.
[38] B. Říhová, K. Ulbrich, J. Strohalm, V. Vetvička, M. Bilej, J. Kopeček, R. Duncan, Biocompatibility of N-2-(hydroxypropyl)methacrylamide copolymers containing adriamycin. Immunogenicity, and effect of haematopoietic stem cells in bone marrow in vivo and mouse splenocytes and human peripheral blood lymphocytes in vitro, Biomaterials 10 (1989) 335–342.
[39] T. Etrych, J. Strohalm, P. Chytil, B. Říhová, K. Ulbrich, Novel star HPMA-based polymer conjugates for passive targeting to solid tumors, J. Drug Target. 19 (2011) 874–889.
[40] D. Fraier, E. Frigerio, E. Pianezzola, M.S. Benedetti, J. Cassidy, P. Vasey, A sensitive procedure for the quantitation of free and *N*-(2-hydroxypropyl)methacrylamide polymer-bound doxorubicin (Pk1) and some of its metabolites, 13-dihydrodoxorubicin, 13-dihydrodoxorubicinone and doxorubicinone, in human plasma and urine by reversed-phase Hplc with fluorometric detection, J. Pharm. Biomed. Anal. 13 (1995) 625–633.
[41] D. Wang, P. Kopečková, T. Minko, V. Nanayakkara, J. Kopeček, Synthesis of starlike *N*-(2-hydroxypropyl)methacrylamide copolymers: potential drug carriers, Biomacromolecules 1 (2000) 313–319.
[42] T. Etrych, L. Kovář, V. Šubr, A. Braunová, M. Pechar, P. Chytil, B. Říhová, K. Ulbrich, High-molecular-weight polymers containing biodegradable disulfide bonds: synthesis and in vitro verification of intracellular degradation, J. Bioact. Compat. Polym. 25 (2010) 5–26.
[43] L.W. Seymour, Y. Miyamoto, H. Maeda, M. Brereton, J. Strohalm, K. Ulbrich, R. Duncan, Influence of molecular weight on passive tumour accumulation of a soluble macromolecular drug carrier, Eur. J. Cancer 31A (1995) 766–770.
[44] P. Rejmanová, J. Kopeček, J. Pohl, M. Baudyš, V. Kostka, Polymers containing enzymatically degradable bonds. 8. Degradation of oligopeptide sequences in N-(2- hydroxypropyl)methacrylamide copolymers by bovine spleen cathepsin B, Makromol. Chem. 184 (1983) 2009–2020.
[45] T. Etrych, L. Kovář, J. Strohalm, P. Chytil, B. Říhová, K. Ulbrich, Biodegradable star HPMA polymer-drug conjugates: biodegradability, distribution and anti-tumor efficacy, J. Control. Release 154 (2011) 241–248.
[46] H. Maeda, J. Wu, T. Sawa, Y. Matsumura, K. Hori, Tumor vascular permeability and the EPR effect in macromolecular therapeutics: a review, J. Control. Release 65 (2000) 271–284.
[47] L.W. Seymour, R. Duncan, J. Strohalm, J. Kopeček, Effect of molecular weight (M_w) of *N*-(2-hydroxypropyl)methacrylamide copolymers on body distribution and rate of excretion after subcutaneous intraperitoneal and intravenous administration to rats, J. Biomed. Mater. Res. 21 (1987) 1341–1358.